First International Conference on Saltwater Intrusion and Coastal Aquifers—
Monitoring, Modeling, and Management. Essaouira, Morocco, April 23–25, 2001

A Finite Volume Unstructured Mesh Method for Modelling Saltwater Intrusion into Aquifer Systems

F. Liu, I. Turner, V. Anh

Queensland University of Technology, Australia

ABSTRACT

Saltwater intrusion occurs in coastal areas worldwide and a theoretical investigation of its sources is crucial because dissolved salts are probably the most common contaminants in freshwater. In the case of coastal aquifers, contamination arises from saltwater invasion, caused primarily by human activities due to heavy urbanisation. Hence, there is a need to predict the location and movement of the saltwater interface to be able to protect freshwater aquifers from the possible danger of contamination. Saltwater intrusion into aquifers presents an extremely complex problem that generally cannot be solved analytically and hence, numerical methods are ideal tools for producing the simulation results.

In this paper, a two-dimensional finite volume unstructured mesh method (FVUM) based on a triangular background interpolation mesh is developed for analysing the evolution of the saltwater intrusion into single and multiple coastal aquifer systems. The model formulation consists of a ground-water flow equation and a salt transport equation. These coupled and non-linear partial differential equations are transformed by FVUM into a system of differential/algebraic equations, which is solved using backward differentiation formulas of order one through five. Simulation results are compared with previously published solutions where good agreement is observed.

INTRODUCTION

The major causes of saltwater intrusion into aquifers are due to the overpumping of coastal areas, excessive pumping in noncoastal regions which overlay saline water bodies, advancement of saltwater through leaky well casings, and natural sources and processes such as drought or tidal variations. Such encroachment obviously limits the usage of groundwater for domestic, agricultural, or industrial purposes. Hence, there is a need to predict the location and movement of the possible danger of contamination fronts. Practical management requires knowledge of not only the present response, but also of the long-term transient response. For these managerial purposes, a numerical model can assist in estimating the location of the freshwater/saltwater interface for given sets of hydrological conditions.

In the past, several numerical models have been proposed to simulate the problem of saltwater intrusion into aquifers. As early as 1964, Henry [1964] developed the first analytical solution for the steady-state salt distribution in a confined coastal aquifer. In many cases, however, a steady-state solution for transient simulations was not obtained due to the high computing costs. Segol, Pinder and Gray [1975] developed the first transient solution based on a velocity-dependent dispersion coefficient using the Galerkin finite element method to solve the set of non-linear

partial differential equations describing the movement of a saltwater front in a coastal confined aquifer. Numerous other researchers, such as Frind [1982], Huyalorn, Andersen, Mercer, Harold and White [1987], Voss [1984] and Cheng, Strobl, Yeh, Lin and Choi [1998] have implemented numerical models for simulating saltwater intrusion problems using a variety of different methods.

The problem of saltwater intrusion into coastal aquifers can be formulated in terms of two tightly coupled, non-linear partial differential equations. The first equation describes the flow of a variable-density fluid, and the second equation describes the transport of dissolved salt. Due to the inherently complex boundary conditions and intricate physical geometries in any practical problem, an analytical solution is not possible. In order to obtain a transient solution, it is necessary to resort to some numerical strategy. This paper presents a finite volume unstructured mesh method (FVUM) for saltwater intrusion into aquifer systems. The solution domain is tessellated with triangles and the control volumes are constructed around the triangle vertices (see Ferguson and Turner, 1996 or more recently Perré and Turner, 1999 for further details). Using this strategy the coupled partial differential conservation equations are discretised into a system of differential/algebraic equations. These equations are then resolved in time according to the backward differentiation formulas that range in order from one through five, depending on the condition of the system. Such temporal integration schemes are known to produce accurate results. These methods are suitable for intricate physical geometries and density-dependent flow and transport through saturated-unsaturated porous media. Simulation results for the case of a confined aquifer are presented and compared with previously published solutions to assess the performance of the newly proposed computational model.

MATHEMATICAL MODEL

The problem of seawater intrusion into aquifers is governed by a coupled non-linear system of two partial differential equations. The first differential equation is the flow equation that describes the head distribution in the aquifer of interest. The classically used pressure head variable employed in the flow equation has been replaced by the use of an equivalent freshwater head that generally results in the elimination of static quantities and improves numerical efficiency.

The flow equation may be written as [Frind, 1982; Huyakorn et al., 1987]:

$$S_s \frac{\partial h}{\partial t} = \nabla \cdot \left[\mathbf{K} \left(\nabla h + \eta C \nabla z \right) \right] \tag{1}$$

where h is the reference hydraulic head referred to as the freshwater head; $\mathbf{K}$ is the hydraulic conductivity tensor; η is the density coupling coefficient; C is the solute concentration; S_s is the specific storage; t is time; z is elevation.

The reference head and the density coupling coefficient in (1) are defined as

$$h = \frac{p}{\rho_0 g} + z \tag{2}$$

and

$$\eta = \frac{\varepsilon}{C_{\max}} \tag{3}$$

where p is the fluid pressure; g is the gravitational acceleration; $C_{\max}$ is the concentration that corresponds to the maximum density $\rho_{\max}$; ρ_0 is the reference (freshwater) density; ε is the density difference ratio defined as

$$\varepsilon = \frac{\rho_{\max}}{\rho_0} - 1. \tag{4}$$

ρ is the density of the mixed fluid (fresh water and saltwater) and the relationship between fluid density and concentration under isothermal conditions can be expressed in the form:

$$\rho = \rho_0 (1 + \eta C) = \rho_0 (1 + \rho_r) \tag{5}$$

where ρ_r is the relative density.

The other differential equation is the transport (dispersion) equation, which is used to describe the chemical concentration. To describe salt transport, we use the following form of the advective-dispersive equation:

$$\phi \frac{\partial C}{\partial t} = \nabla \cdot (\mathbf{D} \nabla C) - \nabla \cdot (C\mathbf{v}) \tag{6}$$

where ϕ is porosity and $\mathbf{D} = \phi \bar{\mathbf{D}}$, with $\bar{\mathbf{D}}$ being the dispersion tensor, whose terms, according to Bear [1979], are defined in a two-dimensional $x - z$ coordinate system as:

$$\begin{aligned} &D_{xx} = \alpha_L \frac{v_x^2}{|\mathbf{v}|} + \alpha_T \frac{v_z^2}{|\mathbf{v}|} + D_d T_{xx}, D_{zz} = \alpha_T \frac{v_x^2}{|\mathbf{v}|} + \alpha_L \frac{v_z^2}{|\mathbf{v}|} + D_d T_{zz}, \\ &D_{xz} = D_{zx} = (\alpha_L - \alpha_T) \frac{v_x v_z}{|\mathbf{v}|} \end{aligned} \tag{7}$$

where α_L and α_T are the longitudinal and transverse dispersivities respectively, D_d is the molecular diffusion coefficient, and T_{xx}, T_{zz} are the principal components of the tortuosity tensor. The Darcy velocity vector may be expressed as

$$\mathbf{v} = -\mathbf{K} (\nabla h + \eta C \nabla z). \tag{8}$$

To obtain a unique solution to (1) and (6), initial and boundary conditions must be specified.

For the flow equation, the initial condition may be expressed as

$$h(x, z; 0) = h_0(x, z) \text{ in } R \tag{9}$$

where R is region of interest; h_0 is the initial head.

The boundary conditions may be stated as follows.

Dirichlet boundary condition:

$$h(x_b, z_b; t) = h_d(x_b, z_b; t) \text{ in } B_d \ . \tag{10}$$

Neumann boundary condition:

$$\mathbf{v} \cdot \mathbf{n} = V_n(x_b, z_b; t) \text{ in } B_n \tag{11}$$

where $\mathbf{n}$ is the outward unit vector normal to the boundary; (x_b, z_b) is a spatial coordinate on the boundary; h_d and V_n are the Dirichlet functional value and Neumann flux, respectively.

For the transport equation, the initial condition may be expressed as

$$C(x, z; 0) = C_0(x, z) \quad \text{in} \quad R. \tag{12}$$

The boundary conditions may be stated as follows.

Dirichlet boundary condition:

$$C(x_b, z_b; t) = C_d(x_b, z_b; t) \text{ in } B_d \ . \quad (13)$$

Neumann boundary condition:

$$n \cdot (-\mathbf{D}\nabla C) = V_n(x_b, z_b; t) \text{ in } B_n \ . \quad (14)$$

Cauchy boundary conditions:

$$\mathbf{n} \cdot (C\mathbf{v} - \mathbf{D}\nabla C) = V_c(x_b, z_b; t) \text{ in } B_c \quad (15)$$

where C_d , V_n and V_c are the Dirichlet functional value , Neumann flux and Cauchy flux, respectively.

A FINITE VOLUME BASED ON TRIANGULAR UNSTRUCTURED MESH METHOD

During the last twenty years there has been a strong focus upon the utilisation of the Finite Volume (FV) or Control Volume (CV) approaches for solving fluid flow and heat transfer problems or, as it is more generally known, problems in Computational Fluid Dynamics (CFD). This success is mostly due to the conservative nature of the scheme and the fact that the terms appearing in the resulting algebraic equations have a specific physical interpretation. In fact, the straightforward formulation and low computational cost compared with other methods have made CV the preferred choice for most CFD partitioners. Over the last ten years, several control volume based-unstructured mesh (FVUM) approaches have in some way overcome the structured nature of the original control volume method [Chow, 1993].

In general, the FVUM methods can be categorised into two approaches, namely, vertex-centred or cell-centred. The classification of the approach is based on the relationship between the control volume and the finite element like unstructured mesh. The approach described here is the vertex-centred, which is more generally known as the Control Volume based Finite Element Mesh method by Baliga and Patankar [1988]. Ferguson and Turner [1996] and Perré and Turner [1999] have used the method for studying the drying of porous media such as wood. In a discrete solution procedure, the solution domain is subdivided into smaller regions and nodes are distributed throughout the domain, the connections between the nodes and the subregions is known as a mesh. In a finite element mesh, the subregions are called elements, with the vertices of the elements being the nodal locations. For the vertex-centred approach only the basic elements are considered, which are three node triangles in this work.

In the solution domain, each node is associated with one control volume. Each surface of the control volume is defined as the vector that joins the centroid of the element to the midpoint of one of its sides as shown in Figure 1. Consequently, each of the triangular elements is divided into three by these control surfaces (CS). These quadrilateral shapes are called sub-control volumes (SCV) and are illustrated in Figure 2. Thus, a control volume consists of the sum of all neighbouring SCVs that surround any given node. The CV is polygonal in shape and can be assembled in a straightforward and efficient manner at the element level. The flow across each control surface must be determined by an integral. The FVUM discretisation process is initiated by utilising the integrated form of the Eqs. (1) and (6). Integrating the flow Eq. (1) and the transport equation (6) over an arbitrary control volume yields:

$$\int_v S_s \frac{\partial h}{\partial t}\, dv = \int_v \nabla \cdot \left[\mathbf{K} \left(\nabla h + \eta C \nabla z \right) \right] dv\,, \tag{16}$$

$$\int_v \phi \frac{\partial C}{\partial t} dv = \int_V \nabla \cdot \left[\mathbf{D} \nabla C \right] dv - \int_V \nabla \cdot \left(C\mathbf{v} \right)\, dv\,. \tag{17}$$

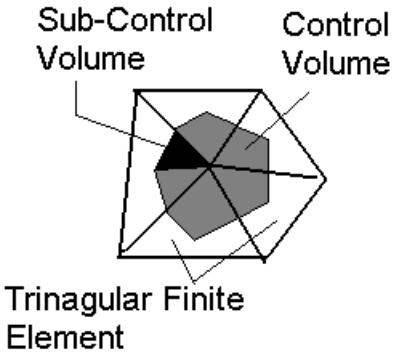

Figure 1: Construction of a control volume from the triangular finite element

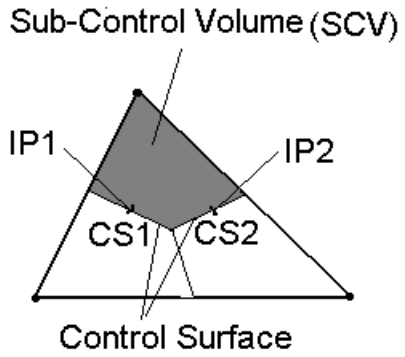

Figure 2: Definition of sub-control volume

Applying the Gauss divergence theorem to the right-hand side of Eqs. (16), (17) and using a lumped mass approach for the time derivative term gives

$$S_p \frac{\partial h_p}{\partial t} v_p = \int_S \left[\mathbf{K} \left(\nabla h + \eta C \nabla z \right) \right] \cdot d\mathbf{n}\,, \tag{18}$$

$$\phi \frac{\partial C_p}{\partial t} v_p = \int_S \left[\mathbf{D} \nabla C \right] \cdot d\mathbf{n} - \int_S \left(C\mathbf{v} \right) \cdot d\mathbf{n} \tag{19}$$

where $d\mathbf{n}$ represents the components of the outward normal surface vector to the control surface S and an anticlockwise traversal of the finite volume integration is assumed, i.e., $d\mathbf{n}$ can be approximated in the discrete sense by $d\mathbf{n} = \Delta z \hat{k} - \Delta x \hat{i}$; Δx and Δz represent the x and z components of the SCV face; v_p is the area of the control volume, and is evaluated for the vertex case as

$$v_p = \sum_{i=1}^{N_{PSCV}} v_{SCV_i} \tag{20}$$

where N_{PSCV} is the total number of SCV's that make up the control volume associated with the node p.

The integrals in Eqs. (18) and (19) are line integrals. These integrals will be approximated by the midpoint approximation for each control surface. To effect this midpoint approximation, the argument of the integrals is required at the midpoint of the control surface and it is for these surfaces that the outward normal vector will be required.

The integral in Eq. (18) can be rewritten as

$$\int_S \left[\mathbf{K} \left(\nabla h + \eta C \nabla z \right) \right] \cdot d\mathbf{n} = \sum_{j=1}^{N_{PSCV}} \int_{S_{j1}+S_{j2}} \left[\mathbf{K}^j \left(\nabla h^j + \eta C^j \nabla z \right) \right] \cdot d\mathbf{n}^j$$

$$= \sum_{j=1}^{N_{PSCV}} \left\{ \sum_{r=1}^{2} \left[\left(K_{x,r}^j \frac{\partial h^j}{\partial x} \Delta z_r^j - K_{z,r}^j \frac{\partial h^j}{\partial z} \Delta x_r^j \right) - K_{z,r}^j \eta C_r^j \Delta x_r^j \right] \right\}. \tag{21}$$

The first integral of the right hand side in Eq. (19) can be rewritten as

$$\int_S \left[\mathbf{D}\nabla C\right]\cdot d\mathbf{n} = \sum_{j=1}^{N_{PSCV}} \int_{S_{j1}+S_{j2}} \left[\mathbf{D}^j \nabla C^j\right]\cdot d\mathbf{n}$$

$$= \sum_{j=1}^{N_{PSCV}} \left\{ \sum_{r=1}^{2} \left[\left(D^j_{xx,r}\frac{\partial C^j}{\partial x} + D^j_{xz,r}\frac{\partial C^j}{\partial z}\right)\Delta z^j_r - \left(D^j_{zx,r}\frac{\partial C^j}{\partial x} + D^j_{zz,r}\frac{\partial C^j}{\partial z}\right)\Delta x^j_r \right] \right\}. \qquad (22)$$

The second integral of the right hand side in Eq. (19) can be rewritten as

$$\int_S C\mathbf{v}\cdot d\mathbf{n} = -\int_S \left[C\mathbf{K}\left(\nabla h + \eta C \nabla z\right)\right]\cdot d\mathbf{n}$$

$$= -\sum_{j=1}^{N_{PSCV}} \int_{S_{j1}+S_{j2}} C^j \left[\mathbf{K}^j\left(\nabla h^j + \eta C^j \nabla z^j\right)\right]\cdot d\mathbf{n}$$

$$= -\sum_{j=1}^{N_{PSCV}} \left\{ \sum_{r=1}^{2} C^j_{r,ups} \left[\left(K^j_x \frac{\partial h^j}{\partial x}\Delta z^j_r - K^j_z \frac{\partial h^j}{\partial z}\Delta x^j_r \right) - K^j_z \eta C^j_{r,S}\Delta x^j_r \right] \right\}. \qquad (23)$$

To evaluate the terms in Eqs. (21), (22) and (23), consider the triangular element, where c_i and b_i are obtained from the anti-cyclic permutation of x and the cyclic permutation of z, respectively. These terms are defined as

$$c_1 = x_3 - x_2, \quad b_1 = z_2 - z_3, \qquad (24a)$$

$$c_2 = x_1 - x_3, \quad b_2 = z_3 - z_1, \qquad (24b)$$

$$c_3 = x_2 - x_1, \quad b_3 = z_1 - z_2. \qquad (24c)$$

The nodal shape functions, which are given in terms of area coordinates, for any point inside Δ_{123} are given by

$$N_i = \frac{A_i}{A}, i = 1,2,3 \qquad (25)$$

where A_i represent the areas of the triangles in the element,

$$A_i = \frac{1}{2}\left(a_i + b_i x + c_i z\right) \qquad (26)$$

with

$$a_1 = x_2 z_3 - x_3 z_2, a_2 = x_3 z_1 - x_1 z_3, a_3 = x_1 z_2 - x_2 z_1 \qquad (27)$$

and A is the area of the triangular element:

$$A = \sum_{i=1}^{3} A_i \,. \qquad (28)$$

Thus, N_1, N_2 and N_3 satisfy the relationship:

$$N_1 + N_2 + N_3 = 1. \qquad (29)$$

Any variable in the element Δ_{123} may be defined if the nodal values are known. Let

$$h = \sum_{i=1}^{3} h_i N_i \,, \qquad C = \sum_{i=1}^{3} C_i N_i \,. \qquad (30)$$

From simple geometry, it can be shown that the derivatives of N_i with respect to x and z are

$$\frac{\partial N_i}{\partial x} = \frac{b_i}{2A}, \quad \frac{\partial N_i}{\partial z} = \frac{c_i}{2A}. \qquad (31)$$

The derivatives of any variable with respect to x and z within the element can be approximated in the same manner as the variable itself:

$$\frac{\partial h}{\partial x}=\sum_{i=1}^{3}\frac{\partial N_i}{\partial x}h_i\,,\qquad \frac{\partial h}{\partial z}=\sum_{i=1}^{3}\frac{\partial N_i}{\partial z}h_i\,, \tag{32}$$

$$\frac{\partial C}{\partial x}=\sum_{i=1}^{3}\frac{\partial N_i}{\partial x}C_i\,,\qquad \frac{\partial C}{\partial z}=\sum_{i=1}^{3}\frac{\partial N_i}{\partial z}C_i\,. \tag{33}$$

If the approximations to the global derivations are used and Eqs. (32) and (33) are substituted into Eqs. (21), (22), (23), the final form of the discretised equations becomes

$$S_s\frac{\partial h_p}{\partial t}v_p = \sum_{j=1}^{N_{PSCV}}\left\{\sum_{r=1}^{2}\left[\sum_{l=1}^{3}\left(K_x^j\frac{\partial N_l^j}{\partial x}\Delta z_{lr}^j-K_y^j\frac{\partial N_l^j}{\partial z}\Delta x_{lr}^j\right)h_l^j-K_y^j\eta C_{r,S}^j\Delta x_{lr}^j\right]\right\}, \tag{34}$$

$$\begin{aligned}\phi\frac{\partial C_p}{\partial t}v_p =& \sum_{j=1}^{N_{PSCV}}\left\{\sum_{r=1}^{2}\sum_{l=1}^{3}\left[\left(D_{xx,r}^j\frac{\partial N_l^j}{\partial x}+D_{xz,r}^j\frac{\partial N_l^j}{\partial z}\right)\Delta z_{lr}^j-\left(D_{zx,r}^j\frac{\partial N_l^j}{\partial x}+D_{zz,r}^j\frac{\partial N_l^j}{\partial z}\right)\Delta x_{lr}^j\right]C_l^j\right\}\\ &+\sum_{j=1}^{N_{PSCV}}\left\{\sum_{r=1}^{2}C_{r,ups}^j\left[\sum_{l=1}^{3}\left(K_x^j\frac{\partial N_i^j}{\partial x}\Delta z_{lr}^j-K_z^j\frac{\partial N_i^j}{\partial z}\Delta x_{lr}^j\right)h_l^j-K_z^j\eta C_{r,S}^j\Delta x_{lr}^j\right]\right\}\end{aligned} \tag{35}$$

where the upstream weighting technique will be used in this work (see Figure 2):

$$C_{r,ups}^j=C_p^j,\ \text{if}\ \ h_p^j\ge h_{p,r}^j\ \ ,\ C_{r,ups}^j=C_{x,r}^j,\ \text{if}\ \ h_p^j<h_{p,r}^j\ . \tag{36}$$

Upstream weighting can be shown to converge to the physically correct solution [Sammon, 1988]. The upstream weighting techniques have been used for saturated-unsaturated flow with dry initial conditions in heterogeneous media (Forsyth, Wu and Pruess, 1995). This strategy has been used here for the flow term concentration in Eq. (35).

The concentration $C_{r,S}^j$ in the gravitational term within each SCV is represented by the use of shape functions at the midpoint ($IPr(x_{IPr},z_{IPr}),r=1,2$) of each SCV, i.e., the $C_{r,S}^j$ will be evaluated at the SCV integration point for each face (see Figure 2):

$$C_{r,S}^j=\sum_{i=1}^{3}C_i^jN_i\left(x_{IPr},z_{IPr}\right). \tag{37}$$

The components of the dispersion tensor will be approximated as

$$\begin{aligned}&D_{xx,r}=\alpha_L\frac{v_{x,r}^2}{|\mathbf{v}_r|}+\alpha_T\frac{v_{z,r}^2}{|\mathbf{v}_r|}+D_dT_{xx},D_{zzr}=\alpha_T\frac{v_{x,r}^2}{|\mathbf{v}_r|}+\alpha_L\frac{v_{z,r}^2}{|\mathbf{v}_r|}+D_dT_{zz},\\ &D_{xz,r}=D_{zx,r}=\left(\alpha_L-\alpha_T\right)\frac{v_{x,r}v_{z,r}}{|\mathbf{v}_r|}\end{aligned} \tag{38}$$

where

$$\left|\mathbf{v}_r\right| = \sqrt{v_{x,r}^2 + v_{z,r}^2}, v_{x,r} = -\sum_{l=1}^{3} K_x^j \frac{\partial N_i^j}{\partial x} \Delta z_{lr}^j h_l^j,$$
$$v_{z,r} = \sum_{l=1}^{3} K_z^j \frac{\partial N_i^j}{\partial z} \Delta x_{lr}^j h_l^j + K_z^j \eta C_{r,S}^j \Delta x_{lr}^j. \quad (39)$$

NUMERICAL SOLUTION STRATEGY

Eqs. (1) and (6) are transformed into a system of ordinary differential equations of the form (34) and (35) for each node using FVUM as described in the above section. In this discretisation, a lumped mass approach and upstream weighting technique have been used. A large number of numerical techniques have been developed for the time-discretisation of this system. In particular, Huyakorn et al. (1987) used the finite difference method, Frind (1982) used a time-weighted form. In this paper, the ordinary differential equations (34) and (35) are solved numerically by using the differential algebraic system solver package DASSL. This program uses the backward differentiation formulas of orders one through five to solve a system of the differential-algebraic equations (Petzold, 1982). The order is selected automatically depending on the condition of the system. Time step control is also adaptive and automatically controlled by the package. The numerical technique has been used to solve adsorption problems involving steep gradients in bidisperse particles (Liu and Bhatia, 1999) and hyperbolic models of transport in bidisperse solids (Liu and Bhatia, 2000).

In order to solve the ordinary differential equations (34) and (35), the boundary conditions must be treated numerically. After assembly of the nodal control volume equations, complete conservation equations will exist for all interior control volumes. However, at solution boundaries, the corresponding control volume will have two control surfaces for which boundary conditions must be applied to complete the equations for conservation. Figure 3 illustrates sub-control volumes for a triangular element where two of its sides form part of the solution domain boundary. In evaluating the boundary conditions along these sides it is necessary to integrate the corresponding boundary control surfaces (BCS) as shown in Figure 3. The usual boundary conditions (10), (11), (13), (14) and (15) can now be easily and directly applied.

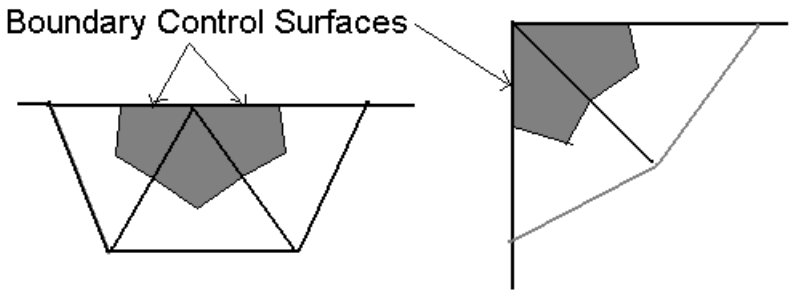

Figure 3: Element boundary and boundary control surfaces

NUMERICAL SIMULATION RESULTS: saltwater intrusion in a confined aquifer

This example concerns groundwater flow and salt transport in a coastal confined aquifer. This example is known widely as Henry's saltwater intrusion problem [Henry, 1959] and is described schematically in Figure 4. The transient analyses were performed. The parameters were chosen so that the cases analyzed correspond to those solved numerically by other researchers [Huyakorn et al., 1987; Cheng et al., 1998]. The boundary conditions employed in our numerical simulation are also shown in Figure 4. The aquifer under consideration is a uniform isotropic aquifer that is bounded below and above by impermeable strata. In addition, the aquifer is exposed on the right side by a stationary saltwater body and is recharged on

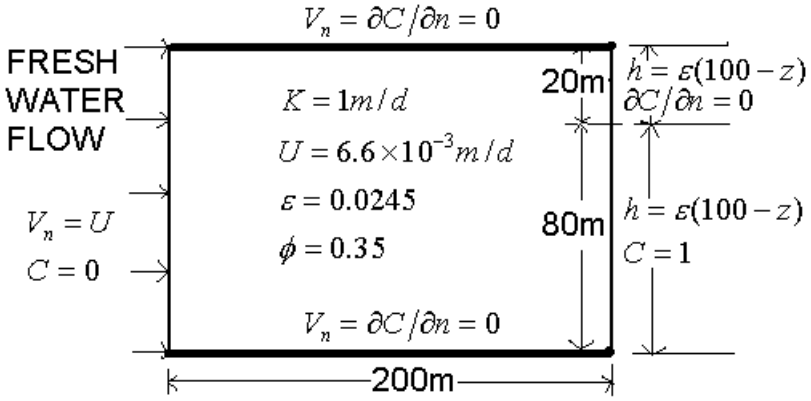

Figure 4: Problem description of saltwater intrusion in a coastal confined aquifer

the left side by a constant freshwater influx. The coastal boundary condition allows convective mass transport out of the system over the top portion $(80m \le z \le 100m)$. Thereupon, the normal concentration gradient is set equal to zero. The initial concentration and reference hydraulic head were set to zero.

The aquifer region was represented by a two-dimensional triangular unstructured mesh consisting of 476 triangular elements and 269 nodes as shown in Figure 5.

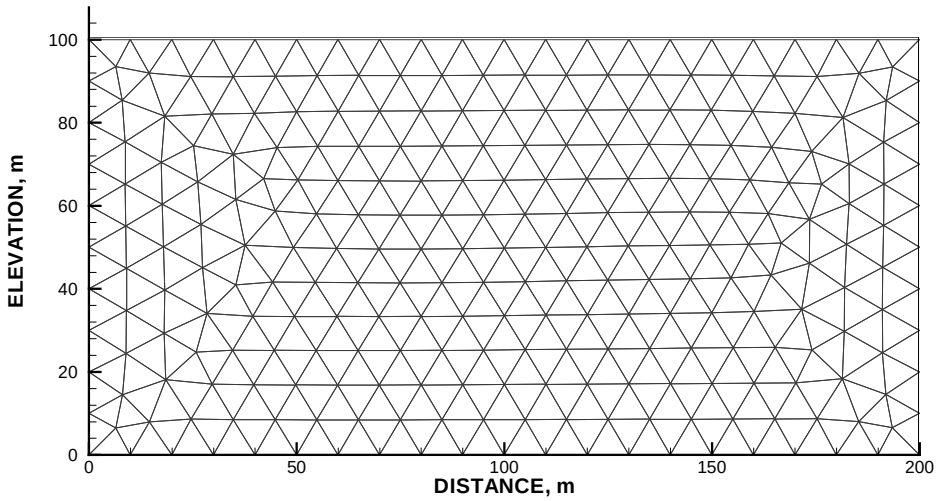

Figure 5: A two-dimensional unstructured mesh

Two cases of variable dispersion and constant coefficients were selected.

For the variable dispersion case, D_d was set to zero, and the longitudinal and transverse dispersivities α_L and α_T were set to 3.5m.

Figures 6 and 7 show the reference head and the 0.5-isochlor distributions using FVUM for the transient state at t=6000 days. It is apparent from Figures 6 and 7 that the present analyses are in good agreement with those of Huyakorn et al. [1987] and Cheng et al. [1998].

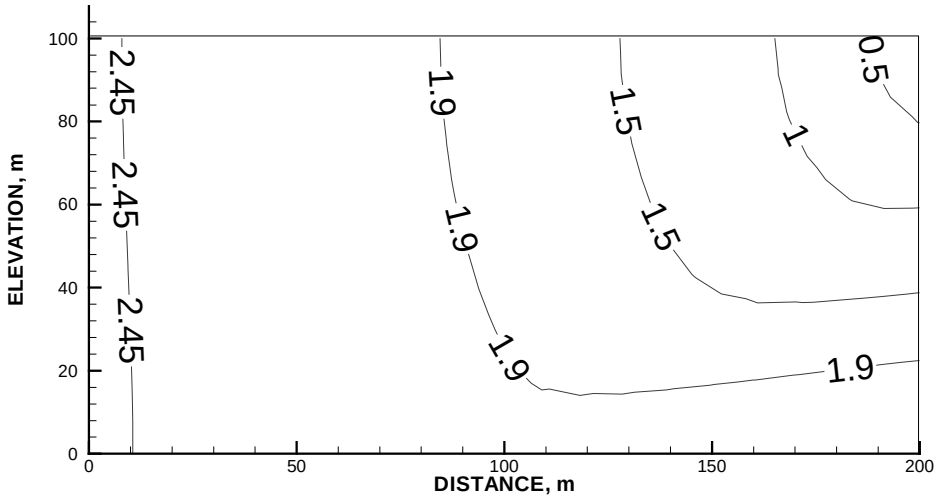

Figure 6: Reference head distribution for transient state at t=6000 days, variable dispersion case

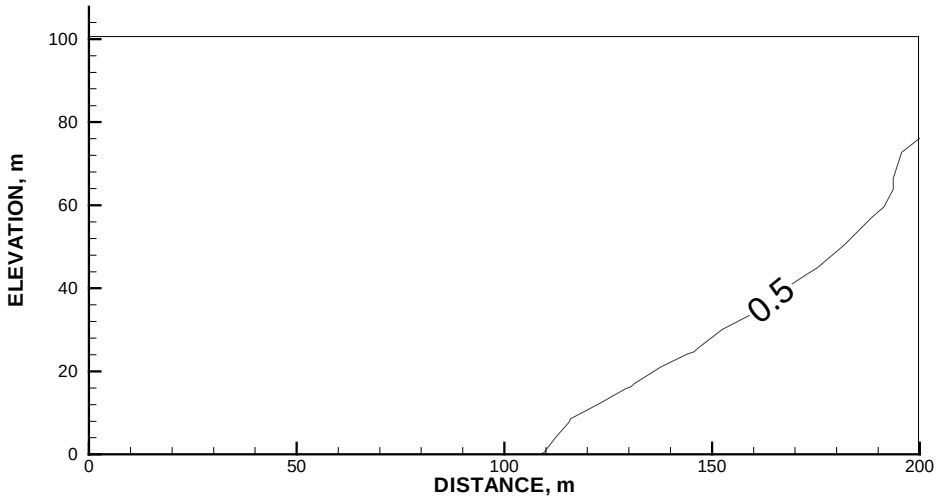

Figure 7: The 0.5-isochlor distribution for transient state at t=6000 days, variable dispersion case

For the constant dispersion case, the molecular diffusion coefficient D_d was set equal to $6.6\times10^{-2} m^2/d$, and the α_L and α_T were set to zero.

Figures 8 and 9 show the reference head and the 0.5-isochlor distributions using FVUM for the transient state at t=6000 days for the constant dispersion case.

It can be observed from these figures that the results are in satisfactory agreement with previously published solutions [Huyakorn et al., 1987; Frind, 1982; Cheng et al., 1998].

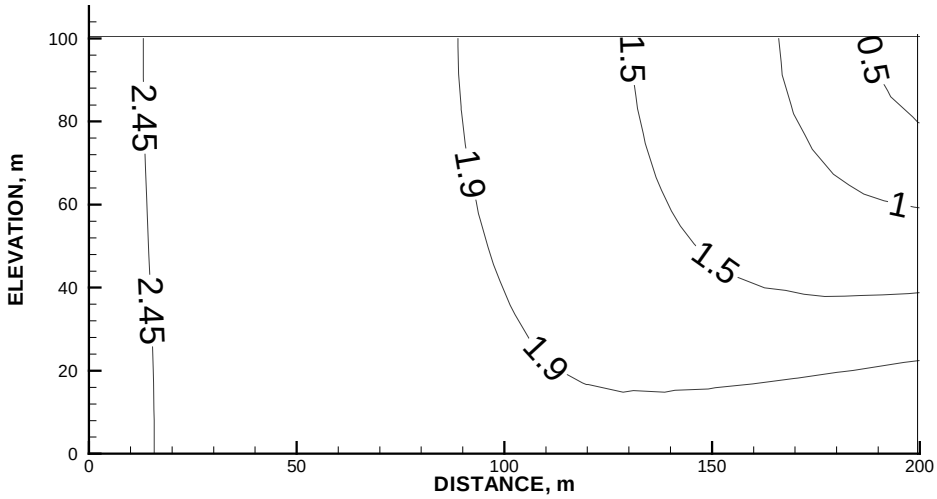

Figure 8: Reference head distribution for transient state at t=6000 days, constant dispersion case

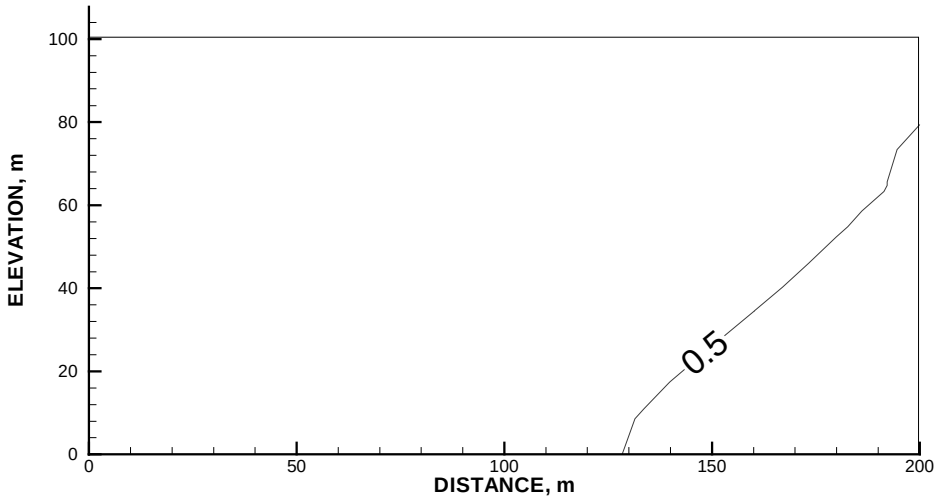

Figure 9: The 0.5-isochlors distribution for transient state at t=6000 days, constant dispersion case

ACKNOWLEDGEMENTS

This research has been supported by the ARC SPIRT grant C10024101.

References

Baliga, B. R. and Patankar, S. V., Elliptic system: finite element I**.** *Handbook of Numerical Heat Transfer*, Editors W. J. Minkowycz et al., pub. Wiley, 1988.

Bear, J., *Hydraulics of Groundwater*, McGraw-Hill, New Your, 1979.

Cheng, J. R., Strobl, R. O., Yeh, G.T., Lin, H.C. and Choi, W. H., "Modeling of 2D density-dependent flow and transport in the subsurface," *J. Hydro. Eng.*, **3(4)**,

248-257, 1998.
Chow, P. M., "Control volume unstructured mesh procedure for convection-diffusion solidification processes," *Ph.D thesis*, University of Greenwich, London, 1993.
Frind, E. O., "Simulation of long-term trasient density-dependent transport in groudwater," *Adv. Water Resour*, **5(2**), 73-88, 1982.
Ferguson, W. J. and Turner, I. W., "A control volume finite element numerical simulation of the Drying of Spruce." *J. Comp. Phys*., 125, 59-70, 1996.
Forsyth, P. A., Wu, Y. S. and Pruess, K., "Robust numerical methods for saturated-unsaturated flow with dry initial conditions in heterogeneous media.," *Adv. Water Resour*, **18**, 25-38, 1995.
Henry, H. R., "Salt intrusion into freshwater aquifers," *J. Geophyd. Res*., **64**, 1911-1919, 1959.
Henry, H. R., "Effects of dispersion on salt encroachment in coastal aquifers, in Sea Water in Coastal Aquifers," (Ed. H. H. Cooper et al.) US Geological Survey Water Supply Paper 1613-C, 1964.
Huyakorn, P. S. Andersen, P. F., Mercer, J.W., and White Jr., H. O., "Saltwater intrusion in aquifers: Develpoment and testing of a three-dimensional finite element model," *Water Resour. Res*.**, 23(2)**, 293-312, 1987.
Liu, F. and Bhatia, S. K., "Computationally efficient solution techniques for adsorption problems involving steep gradients in bidisperse particles," *Comp. Chem. Eng*., **23**, 933-943, 1999.
Liu, F. and Bhatia, S. K., "Numerical solution of hyperbolic models of transport in bidisperse solids." *Comp. Chem. Eng*., **24**, 1981-1995, 2000.
Pelzold, L. R., A description of DASSL: a differential/algebraic equation system solver, *Technical Report No. SAND 82-8637*, Sandia National Laboratories, Livermore, 1982.
Perré P. and Turner I., TransPore: A Generic Heat and Mass Transfer Computational Model for Understanding and Visualising The Drying Of Porous Media, Invited paper, Drying Technology Journal, **17(7)**, 1273-1289, 1999a.
Patankar, S. V., *Numerical Heat Transfer and Fluid Flow*, McGraw-Hill, New Your, 1980.
Segol. G., Pinder, G. F. and Gray, W. G. (1975) "A galerkin finite element technique for calculating the transient position of the saltwater front." *Water Res*., **11(2)**, 343-347, 1975.
Sammon, P., "An analysis of upstream weighting," *SPE J. RES. Eng*., **3**, 1053-1056, 1988.
Voss, C.I., AQUIFEM-SALT: A Finite-element model for aquifers containing a seawater interface, USGS Water Resour. Invest. Rpt. 84-4263, 1984a.

Keywords: Control Volume, unstructured mesh, transient simulation, upstream weighting

Corresponding auther: Fawang Liu, School of Mathematical Sciences, Queensland University of Technology, GPO Box 2434, Brisbene, Qld. 4001, Australia. Email: f.liu@fsc.qut.edu.au.